NATURA SLOVENIAE 25(3): 213-237
NERETVA SCIENCE WEEK 2022 – SCIENTIFIC PAPER

Prejeto / Received: 15. 3. 2023
Sprejeto / Accepted: 16. 6. 2023

DOI: 10.14720/ns.25.3.213-237

Differential controls on CO_2 and CH_4 emissions from the free-flowing Neretva River, Bosnia and Herzegovina

Martin DALVAI RAGNOLI, Thea SCHWINGSHACKL, Serafine KATTUS, Julius LISSY, Elisabeth WENINGER, Gabriel SINGER

Department of Ecology, University of Innsbruck, 6020 Innsbruck, Austria. Correspondence: Martin Dalvai Ragnoli; E-mails: martin.dalvai-ragnoli@uibk.ac.at and Gabriel Singer; E-mail: gabriel.singer@uibk.ac.at

Abstract. Streams and rivers emit methane (CH_4) and carbon dioxide (CO_2), two greenhouse gasses contributing to global warming. Estimates for diffusive gas emissions can be obtained by multiplying the concentration gradient between water and atmosphere with the gas transfer velocity. The latter is purely physically constrained, yet spatially highly variable. And - in a flowing water ecosystem - the local concentration gradient is the result of a dynamic balance between upstream evasion and resupply. The collection of representative emission data is thus challenging and emissions of river ecosystems are rarely assessed considering temporal variability and spatial dependence at network scale. In this study, we uncover spatial heterogeneity and controls of concentrations and emission fluxes of the two greenhouse gasses, CH_4 and CO_2, along a 50 km length of a pristine river system, the Neretva River in Bosnia and Herzegovina. This remote river network has so far remained barely influenced by human activities and the hydromorphological status is to date not altered. The Neretva can therefore serve as a reference for similar systems in the region. This seems to be particularly important as rivers in the Western Balkans, including the Neretva, are currently experiencing a surge in hydropower development and damming, which is known to strongly affect riverine greenhouse gas emissions. We found high emissions as a result of co-occurrence of high concentration with high exchange velocity, but we identified different underlying mechanistic processes driving the evasion of the two gasses. CH_4 was strongly supply-limited: elevated concentrations were exclusively measured in a large pool (0.84 µmol L^{-1} compared to a median concentration of 0.005 µmol L^{-1} in the entire study section). This resulted in CH_4 evasion being four orders of magnitude higher in the turbulent reach following the pool (22 mmol m^{-2} d^{-1}) compared to the median evasion at network scale (0.06 mmol m^{-2} d^{-1}). In contrast, CO_2 evasion was more variable in time and equally dependent on CO_2 and gas exchange velocity. The construction of dams intended in this area would lead to reservoirs of slowly flowing or standing water with similar habitat conditions as the observed CH_4-hotspot. The concomitant increase in residence time and higher retention of organic material will lead to an increase of CH_4 production replacing aerobic respiration. Consequently, CH_4 emissions can be expected to drastically increase by orders of magnitude. This greenhouse gas footprint of hydropower generation may counteract the promised climate benefits in terms of renewable energy production.

Key words: dams, gas transfer velocity, greenhouse gas, greenhouse gas footprint of hydropower, emission fluxes, pristine reference river

Izvleček. Različni mehanizmi kontrol emisij CO_2 in CH_4 iz prostotekoče reke Neretve v Bosni in Hercegovini – Potoki in reke oddajajo metan (CH_4) in ogljikov dioksid (CO_2): toplogredna plina, ki prispevata h globalnemu segrevanju. Ocene difuzne emisije plinov izračunamo tako, da zmnožimo koncentracijski gradient med vodo in atmosfero ter hitrost prenosa plina. Slednja je izključno fizikalno omejena, vendar prostorsko zelo spremenljiva. Lokalni koncentracijski gradient v tekočem vodnem ekosistemu je rezultat dinamičnega ravnovesja med izgubo vodika in ponovnim polnjenjem. Zato je zbiranje reprezentativnih podatkov o emisijah zahtevno opravilo, ocene emisij rečnih ekosistemov pa le redko upoštevajo časovno spremenljivost in prostorsko odvisnost na ravni celotne mreže. Študija analizira prostorsko heterogenost in kontrolne mehanizme koncentracij in emisijskih tokov toplogrednih plinov CH_4 in CO_2 vzdolž 50 km dolgega odseka neokrnjenega rečnega sistema reke Neretve v Bosni in Hercegovini. Ta odročni del rečnega sistema do sedaj skorajda ni bil izpostavljen človekovim posegom in je, za zdaj, hidromorfološko še vedno nespremenjen v prvotnem naravnem stanju. Zgornja Neretva zato lahko rabi kot referenca za podobne sisteme v regiji. To je še posebej pomembno, saj se na rekah zahodnega Balkana, vključno z Neretvo, trenutno hitro razvija hidroenergetika in gradijo jezovi, ki znatno vplivajo na emisije toplogrednih plinov iz rek. V študiji smo odkrili visoke emisije, ki so posledica hkratnega pojavljanja visoke koncentracije in visoke izmenjave. Identificirali smo različne mehanistične procese, ki vodijo do emisij obeh plinov. CH_4 je bil močno omejen na viru: povišane koncentracije smo izmerili izključno v velikem bazenu (0,84 µmol L^{-1} v primerjavi s srednjo koncentracijo 0,005 µmol L-1 v celotnem odseku). Posledično so bile emisije CH_4 v turbulentnem delu, ki sledi bazenu, višje za kar velikostne razrede (22 mmol m^{-2} d^{-1}), v primerjavi s srednjimi emisijami na ravni celotnega omrežja (0,06 mmol m^{-2} d^{-1}). Nasprotno pa je bila emisija CO_2 bolj časovno spremenljiva in enako odvisna od koncentracije CO_2 in hitrosti izmenjave le tega. Načrtovana gradnja jezov na tem območju bi vodila do rezervoarjev počasi tekoče ali stoječe vode s podobnimi habitatnimi razmerami, kot so bili opaženi na vroči točki CH_4. Spremljajoče povečanje časa zadrževanja in večje zadrževanje organskega materiala bo vodilo do povečano proizvajanje CH_4, ki bo zamenjalo aerobno dihanje. Posledično lahko pričakujemo, da se bodo emisije CH_4 drastično povečale. Toplogredni odtis proizvodnje hidroenergije bo tako najverjetneje izničil obljubljene podnebne koristi v smislu proizvodnje obnovljive energije.

Ključne besede: toplogredni plin, emisijski tokovi, hitrost prenosa plina, neokrnjena referenčna reka, jezovi, toplogredni odtis hidroelektrarn

Apstrakt. Različiti mehanizmi kontrole emisija CO_2 i CH_4 iz slobodnotekuće rijeke Neretve, Bosna i Hercegovina – Ekosistemske funkcije su okosnica usluga ekosistema koje rijeke pružaju ljudskim zajednicama. Funkcionisanje ekosistema proizlazi iz interakcije između bioloških zajednica i njihovog okruženja. Pošto se uslovi životne sredine u rijekama mijenjaju duž njihovog longitudinalnog kontinuma, mijenja se i funkcionisanje. Ponekad ove promjene ne prate glatke gradijente već velike diskontinuitete. Ovo može biti slučaj u krečnjačkim, kraškim rijekama zbog iznenadnih masivnih unosa podzemnih voda duž pejzaža, što je tipičan fenomen za balkanske rijeke. Uprkos velikom geodiverzitetu i velikoj ekološkoj vrijednosti, balkanske rijeke su i dalje nedovoljno istražene. Ovdje smo istražili kako funkcioniše ekosistem i njihova raznovrsnost (procijenjena kao multifunkcionalnost) se mijenja duž kontinuma kraške rijeke Neretve koja slobodno teče u Bosni i Hercegovini. U tu svrhu izmjerili smo podskup osnovnih funkcija ekosistema (bruto primarna proizvodnja ekosistema, neto primarna proizvodnja biofilma i enzimske aktivnosti, razgradnja organske materije) u jedanaest riječnih tokova od izvora Neretve do riječnih dijelova uzvodno od akumulacije Jablanica. Otkrili smo da su različite funkcije dostigle svoj maksimum u različitim dijelovima Neretve zavisno o unosu hranjivih materija. Dok je razgradnja organske materije bila najveća u glavnim vodama zbog unosa nutrijenata iz priobalne vegetacije, enzimska aktivnost biofilma je imala najveće vrijednosti u srednjim dijelovima zbog unosa NH^{4+}-N u podzemne vode, a primarna proizvodnja je bila najveća u većini nizvodnih dijelova zbog akumulacije NO^{3-}-N i PO_4^{3-}-P sa slivnom površinom. Kao rezultat toga, prosječna multifunkcionalnost je dostigla vrhunac na lokacijama s najvećom koncentracijom nutrijenata preko kontinuma rijeke Neretve, što ukazuje na jači uticaj unosa nutrijenata od položaja mreže. Iskonski uslovi Neretve rezultiraju oligotrofnim uslovima duž njenog gornjeg toka. Naši rezultati naglašavaju veliku osjetljivost funkcionisanja ekosistema u Neretvi na unos nutrijenata i ekološkog diskontinuiteta, bilo prirodne ili ljudske. Potencijalni veliki, dugoročni uticaji na područje mogu promijeniti postojeće gradijente životne sredine, a time i funkcionisanje ekosistema u rijekama na lokalnom i regionalnom nivou.

Ključne riječi: staklenički plinovi, emisijski tokovi, brzina prenosa gasa, netaknuta referentna rijeka, brane, staklenički plinovi iz hidroelektrana

Introduction

Streams and rivers are important sources of gaseous carbon to the atmosphere. Out-gassing of carbon from streams to the atmosphere occurs mostly in the form of methane (CH4) and carbon dioxide (CO2), which are also the two most important greenhouse gasses (GHG) contributing to global warming (Aufdenkampe et al. 2011; Stanley et al. 2016). A recent estimate suggests global carbon out-gassing from inland waters amounts to 3.9 PgC yr^{-1} (Drake et al. 2018), where streams and rivers may be responsible for more than 85% of CO_2 (Raymond et al. 2013) and for 50% of CH4 (Stanley et al. 2016) evasion. However, emissions from streams and rivers are considered to not be well quantified on a global scale (Hotchkiss et al. 2015; Lupon et al. 2019) as substantial uncertainties remain due to the heterogeneity, temporal variability and badly constrained surface areas of small headwaters. Rivers are also highly dynamic systems and difficulties associated with continuous monitoring hinder collection of representative emission data. Taken together, uncertainties to estimate global surface area of streams and rivers, lack of dissolved gas concentration measurements and gas transfer velocity measurements still hinder accurate global upscaling of gas emissions. Especially small streams and rivers are under-represented in literature; yet, these appear to have the highest gas exchange velocities, often also the highest CO_2 partial pressures, and highest surface-to-volume ratios (Aufdenkampe et al. 2011; Butman & Raymond 2011; McGinnis et al. 2016).

Aquatic gas evasion in streams can vary at the scale of meters. Besides the partial pressure of a gas in the water phase, evasion is regulated by physical processes linked to water turbulence, which determine the vertical gas transfer velocity (k; m d^{-1}) (Crawford et al. 2013). Current upscaling approaches mostly use estimates of gas partial pressure at a large scale combined with a finer scaled estimate of gas transfer velocity, thereby poorly accounting for actual process variability at small spatial scale (Crawford et al. 2017; Duvert et al. 2018). More importantly, the resulting flux estimates, achieved by multiplication of a concentration term and the gas transfer velocity, may be erroneous as these two variables are not independent from each other in flowing water ecosystems: gas concentration is the result of a dynamic balance between resupply to the system versus evasion (Rocher-Ros et al. 2019). Depending on the limiting factor, gas evasion can be either supply-limited or transfer-limited. While the former happens at low concentrations, the latter happens in sections with low gas transfer velocities (Rocher-Ros et al. 2019).

CO_2 can be produced and consumed by in-stream processes: the production of CO_2 by heterotrophs is counteracted by the consumption of CO_2 by primary producers. This means that CO_2 concentration may be subject to widespread day-night changes because of the absence of photosynthetic activity at night (Peter et al. 2014; Gómez-Gener et al. 2021). While organic matter is preferentially degraded through aerobic respiration, anaerobic pathways are not unusual. In fact, some studies report the potential for benthic in-stream CH_4 production in anoxic sediments with enhanced organic content (Crawford & Stanley 2016). In the presence of anoxic (or generally low-redox) microzones, aerobic CO_2 and anaerobic CH_4 production may occur simultaneously in the streambed sediment (Baker et al. 1999). This way, CH_4 resulting from CO_2 reduction has even been observed in oxygenated headwater streams (Flury & Ulseth 2019). Notably, in-stream produced CH_4 may be quickly consumed by methanotrophic bacteria, which use this highly reduced organic compound as energy and carbon source in zones well supplied with oxygen (Bastviken 2009; Stanley et al. 2016). Indeed, high methane oxidation rates typically substantially depress otherwise high methane emissions (Bastviken 2009).

GHGs, however, also originate from surrounding ecosystems, specifically soils and groundwater, and can be delivered to streams by subsurface soil flow paths or by groundwater input (Lupon et al. 2019). Groundwater input, which is a key connection between terrestrial and aquatic environments (Leach et al. 2017), is often characterised by a change in stream water chemistry (Horgby et al. 2019) as it can deliver large amounts of carbon (DIC, DOC and gaseous C) to the stream (Crawford et al. 2015; Duvert et al. 2018; Ledesma et al. 2018; Lupon et al. 2019). Thereby, sourced organic carbon can be respired within a very short distance (Rasilo et al. 2017), supporting high mineralisation rates and elevated concentrations in carbon gases (Horgby et al. 2019). Groundwater input also directly brings carbon gases, which may quickly outgas from small streams with high gas exchange velocities. This combination of localised input and outgassing can create notably small-scale spatially variable concentrations of CO_2 and CH_4 (Lupon et al. 2019). Such point source inputs with chemically distinct properties and which potentially result in local hot spots for GHG emissions, may be of particular importance in streams draining karstic terrain, where underground flow paths can be long and water reaches rivers predominantly through high-volume springs (Valdes et al. 2007; Operta & Pamuk 2015).

The goal of our study was to investigate CH_4 and CO_2 concentrations and assess the drivers of respective emission fluxes along the continuum of the upper course of the Neretva River in Bosnia-Herzegovina. This river section is characterised by high landscape diversity, including upland forested reaches with limited alder-covered floodplains, several steep canyon reaches, and a meandering alluvial reach where multiple channels appear. Anthropogenic influence, however, is minimal, making this river section a potential reference for similar systems in the region. The river is further influenced by multiple spatially discontinuous inputs of karstic springs that can reach substantial discharge. Thus, the studied river section presents itself as a naturally heterogeneous river system, where ecological concepts describing river continua are challenged and the existing discontinuities of river morphology, lateral input and in-stream functioning may dominate fluxes of CO_2 and CH_4. Consequently, we expect a high spatial variation in dissolved gas concentration and spatially distinct hotspots of CO_2 and CH_4 related to karstic inputs. We further expect spatial patterns to not overlap between the two gases, reflecting that underlying processes and drivers for emission fluxes along this free-flowing river section are not identical for CO_2 and CH_4.

Material and methods

Study area and study design

The Neretva has a catchment size of more than 10,000 km^2 and flows from the Dinaric Alps in Bosnia and Herzegovina into the Adriatic Sea in Croatia over a length of 220 km (Djedjibegovic et al. 2010). We studied 50 km of the upper course of the Neretva River from the Krupac confluence (10 km upstream of the village of Ulog, (43°19'20.5"N, 18°26'02.4"E) until a point upstream of the Jablanica reservoir near Konjic (43°37'55.4"N, 17°59'58.3"E). The hydromorphological status of the upper Neretva River is defined as near natural (Chamberlain

2018) and human influence is minimal due to the absence of big settlements and industrial areas.

Hydrogeologically, the studied section of the Neretva River can be divided into two parts: The stretch upstream of Ulog is characterised by fissured aquifers with low permeability, whereas the section downstream of Ulog until Konjic contains karst aquifers of high permeability (Grego 2020). The mean annual flow rate amounts to roughly 9 $m^3 s^{-1}$ in Ulog and to about 58 $m^3 s^{-1}$ in Konjic (DIKTAS B & H 2012).

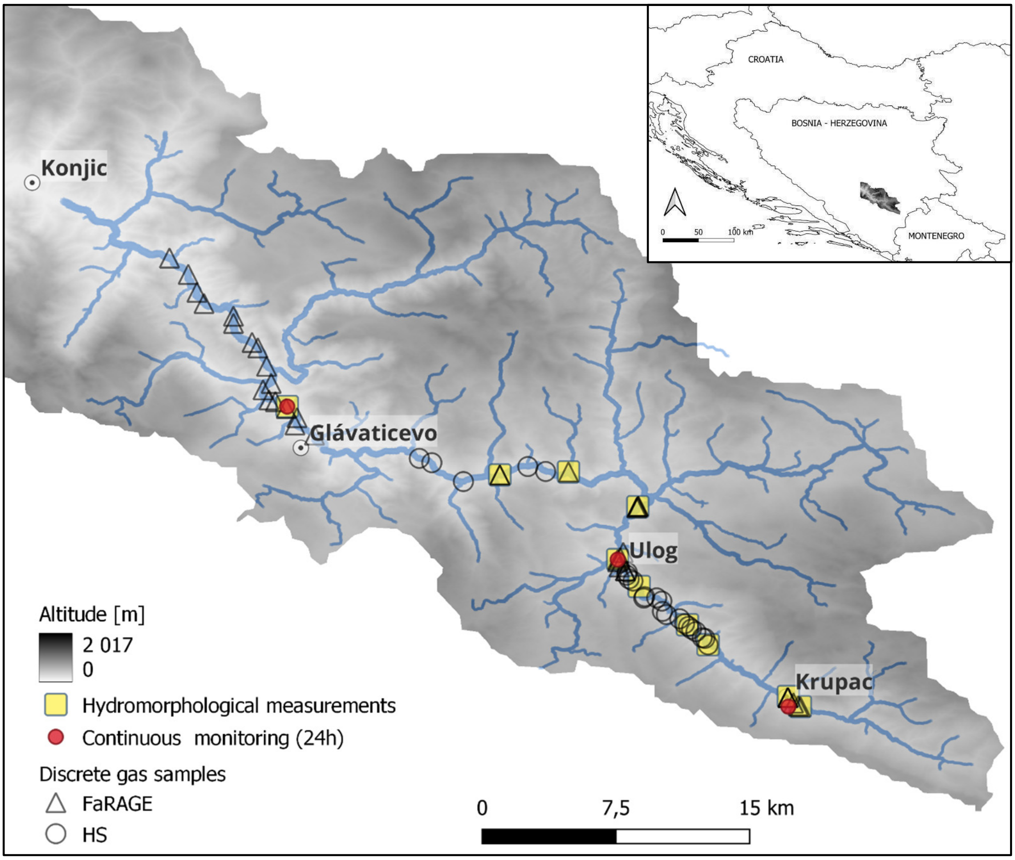

Figure 1. Studied section of the upper Neretva River. Here shown are sampling sites for hydromorphological measurements, the sites selected for continuous monitoring over 24 h and sites used for discrete gas samples. The latter were either performed with the self-built equilibration system (FaRAGE) or with the headspace technique (HS). Major settlements Konjic, Glavatičevo and Ulog are highlighted as well as the confluence of the Krupac tributary.

Slika 1. Preučevani odsek zgornje Neretve. Prikazana so vzorčišča za hidromorfološke meritve, mesta, izbrana za neprekinjeno 24-urno spremljanje, in mesta, uporabljena za posamične vzorce plina. Zadnje smo opravili z lastno izdelanim ekvilibracijskim sistemom (FaRAGE), ali pa z metodo plinske faze (HS). Izpostavljena so glavna naselja Konjic, Glavatičevo in Ulog ter sotočje pritoka Krupac.

Slika 1. Proučavani dio gornjeg toka rijeke Neretve. Ovdje su prikazana mjesta uzorkovanja za hidromorfološka mjerenja, mjesta izabrana za kontinuirano praćenje tokom 24 sata i mjesta korištena za uzimanje diskretnih uzoraka plina. Ovi posljednji su obavljeni ili sa samostalno izgrađenim sistemom za ekvilibraciju (FaRAGE) ili tehnikom faze plina (HS). Naglašena su i glavna naselja Konjic, Glavatičvo i Ulog, kao i ušće pritoke Krupac.

During a ten-day field campaign in July 2022, we performed single point measurements of dissolved CH_4 and CO_2 at 60 sites (Fig. 1). In addition to these measurements taken at arbitrary time points during daylight hours (from 08:00 to 18:00), we took three series of discrete single point measurements spread over 24 h at three selected sites.

Hydromorphology and auxiliary field data

At ten sites spanning the entire study section (Fig. 1), we measured discharge and characterised the river's morphology. For discharge (Q), we measured depth (d) and flow velocity (v) at a minimum of ten regularly spaced (0.5-2.5 m) locations along a cross-section with measured width (w). Flow velocity was measured at 40% depth using a flow meter (FlowSens, SEBA Hydrometrie, Germany). Discharge was then calculated as the product of width, average depth and average flow velocity. At site 1, which was located after a confluence, we calculated discharge from the measured discharge of one tributary and conductivities at both tributaries and the mainstem by mass balance. Additionally, at each of these ten sites, we selected a 50-meter-long river reach to measure depth and flow velocity representing a river's average morphological character better than a single cross-section. To randomise sampling points, we walked from shore to shore in a zig-zag pattern and took a total of 15-50 measurements every three steps.

Catchment area and slope at network scale were derived from a digital elevation model (Copernicus 2022) with a resolution of 30 meters using the R package *watershed* (Talluto 2020) for delineation of the watershed. Hydraulic parameters used for computation of k_{600} at reach-scale were derived from hydraulic scaling relations for river depth (d) and flow velocity (v) as functions of discharge (Leopold et al. 1964):

$$d = c_d Q^{e_d} \tag{1}$$
$$v = c_v Q^{e_v} \tag{2}$$

Parameters of these power law relationships were obtained by fit to hydraulic measurements and compared with values reported in literature. To predict discharge, we used a simple linear model of measured Q to catchment area, which in turn is derived from a digital elevation model (DEM).

Surface water temperature, conductivity, dissolved oxygen, and pH were measured using a WTW handheld probe (Xylem, Weilheim, Germany) at 10 cm depth of a well-mixed location. Additionally, a water sample was taken at the 10 main sites to characterise the chemical composition of the surface water for dissolved organic carbon (DOC) and nutrient concentration. Methods for water chemical analysis are described in detail elsewhere (Del Campo et al., this issue).

Dissolved gas concentration

We used two different methods to measure dissolved gas concentrations of CO_2 and CH_4. The headspace technique was used to measure grab samples collected at remote locations and during the continuous monitoring of gas concentrations over time, at three sites. The equilibrator-based method, which is needed for *in-situ* application of the measuring instrument, was used for easily accessible locations and for sampling from a raft in the lower sections of the study area. Gas concentration was always measured using a micro portable greenhouse gas analyser (MGGA, Los Gatos Research, USA). The MGGA uses laser absorption spectroscopy and detects CO_2 and CH_4 with a precision of 6 ppm and 4 ppb, respectively.

We computed gas saturation using local measurements of water temperature and atmospheric pressure as well as the mean of CO_2 and CH_4 atmospheric background concentration measured at arbitrary locations and points in time during our sampling campaign.

To measure concentrations of CH_4 and CO_2 by the headspace technique, samples were taken with a 60 mL syringe by collecting 30 mL of water from 10 cm below the water surface and filling up the syringe with background air (30 mL). To enhance equilibration between both phases the syringe was intensely shaken for approximately two minutes. From the gaseous headspace approximately 25 mL were transferred into pre-evacuated 20 mL gas vials and stored with overpressure until further analysis. The MGGA was then used in an environment with stable temperature and pressure conditions to measure small sample volumes in a closed-loop configuration (Wilkinson et al. 2018). After temperature acclimation and pressure equalisation to local conditions, the gas vials were directly measured by incorporating them into the closed loop using three-way valves (Fig. 2). This closed loop method requires consideration of sample dilution by ambient gas inside the loop by calculating a volume ratio between sample volume and loop volume. For this purpose, a sample of gas standard with known gas composition was analysed at *in-situ* pressure and temperature conditions. From the resulting headspace concentration, the equilibrium concentration of the water phase was computed using Henry's law of solubility. The original water concentration is finally computed by summing the number of moles in the equilibrated phases and accounting for the background concentration. Detailed computation steps can be found in the supplementary information.

To measure dissolved CO_2 and CH_4 concentration *in-situ*, we built a fast equilibrator similar to the Fast-Response Automated Gas Equilibrator (FaRAGE) described by Xiao et al. (2020). This flow-through system equilibrates a continuous flow of fresh water with a small closed volume of air and allows continuous measurement of dissolved gas concentrations. We modified the original FaRAGE system to better suit our needs, specifically higher portability and lower maintenance and application costs (Fig. 2). Briefly, water from the river is continuously pumped into the system using a peristaltic pump (Eijkelkamp, Netherlands). The water phase is mixed in the mixing unit with an internally recirculated gas phase. Gas bubble size is decreased using a pumice stone. After mixing, the gas-water mixture travels through a coiled tubing (2 m length) to enhance equilibration. Degassing occurs at the separation unit, when the mixture enters a chamber with a larger diameter and the flow velocity is decreased. From there, water is discharged back into the river by flowing freely downwards. The gas phase, however, is recirculated in a closed loop by sending it back to the mixing unit using a gas-tight membrane pump. From the separation unit a gas sample is drawn using the flow rate of the MGGA, bypassed through the analyser to continuously measure the gas concentration, and returned to the separation unit. During use, this equilibrator system was submerged in the river to allow equilibration at water temperature.

Complete equilibration is reflected in a stable concentration plateau measured by the MGGA. All gas calculations are hereafter explained for CH_4, but work analogously for CO_2. Dissolved gas concentration can be directly computed from equilibration concentration by applying Henry's law of solubility:

$$C_{CH_4\,w} = p_{CH_4} KH_{CH_4}(T_w) \quad (3)$$

Where $C_{CH4\,w}$ is the dissolved concentration of CH_4 (mol L^{-1}), p_{CH4} the partial pressure (atm) computed from the molar fraction measured (in ppm) by the MGGA and the ambient pressure, and KH_{CH4} the temperature dependent Henry constant (mol L^{-1} atm^{-1}). KH can be calculated for CO_2 and CH_4 according to IHA (IHA 2010). In the field, ambient pressure was measured using a multifunctional watch (Suunto core, Finland) and water temperature was measured with the WTW handheld probe (Xylem, Weilheim, Germany).

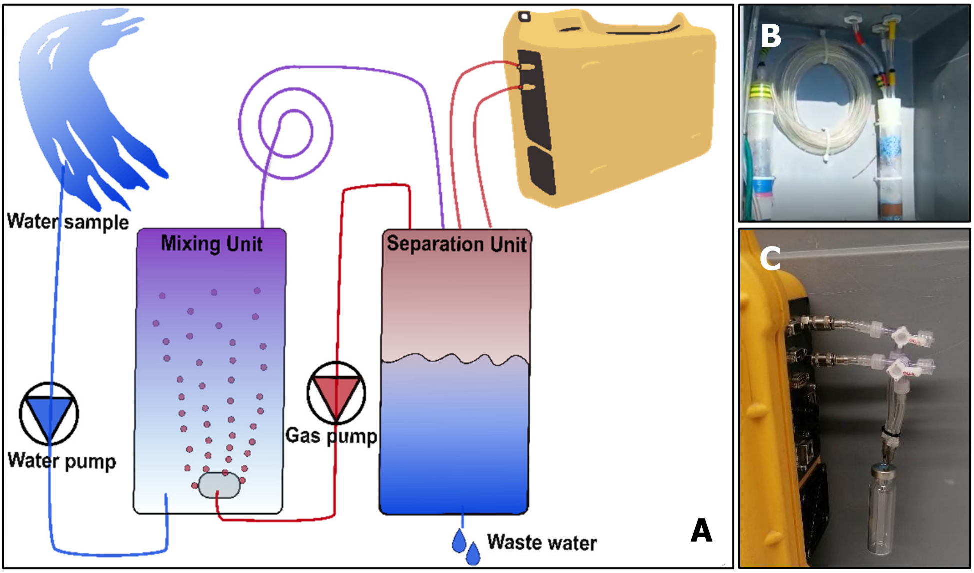

Figure 2. Schematic illustration of the equilibrator system (A): main components are a water pump, a mixing unit, a separation unit, a gas pump and the MGGA. The red colour marks the flow of the gaseous head space, blue the water flow and purple the gas-water mixture. Picture of the mixing unit and separation unit of the equilibrator system (B) and picture of the used closed loop system for headspace samples (C).

Slika 2: Shematski prikaz ekvilibracijskega sistema (A): Glavne komponente so vodna črpalka, mešalna enota, separacijska enota, plinska črpalka in MGGA. Rdeča barva označuje tok plinske faze, modra vodni tok, vijolična pa mešanico plina in vode. Slika mešalne enote in separacijske enote ekvilibracijskega sistema (B) ter slika uporabljenega zaprtega sistema za vzorce plinske faze (C).

Slika 2: Šematski prikaz sistema ekvilibratora (A): Glavne komponente su vodena pumpa, jedinica za mješanje, separacijska jedinica, plinska pumpa i MGGA. Crvena boja označava tok gasne faze, plava boja tok vode, a ljubičasta boja mješavinu gasa i vode. Slika jedinice za mješanje i separacijske jedinice sistema ekvilibratora (B) i slika korištenog zatvorenog sistema za uzimanje uzoraka faze plina (C).

Calculation of GHG flux to the atmosphere

The diffusive gas flux can be calculated for known dissolved gas concentration according to:

$$F_{CH_4} = k_{CH_4} \left(C_{CH_4\,w} - C_{CH_4\,EQ}\right) \tag{4}$$

Here, F_{CH4} is the gas flux of CH_4 (mol m^{-2} d^{-1}), k_{CH4} the gas exchange velocity (m d^{-1}), $C_{CH4\ W}$ the measured dissolved gas concentration (mol L^{-1}), and $C_{CH4\ EQ}$ the hypothetical gas concentration that the water phase would have in complete equilibrium with the ambient air (mol L^{-1}). The latter can be computed from the water temperature and the atmospheric partial pressure using Henry's law of solubility. The gas transfer velocity can be computed for any gas and temperature from the standardised gas transfer velocity (k_{600}) and Schmidt number scaling (Raymond et al. 2012):

$$k_{CH_4} = k_{600} \cdot \left(\frac{600}{Sc_{CH_4}(T_W)}\right)^{0.5} \tag{5}$$

Here, the Schmidt number is calculated with the water temperature and given the specific parameterisation of Raymond et al. (2012), the exponent of 0.5 is commonly used for turbulent water (Jähne et al. 1987). k_{600} was estimated by an ensemble-modelling approach from channel hydraulics (i.e., stream velocity, slope, depth and discharge) using the average of predictions of equations 1-7 in Raymond et al. (2012), the necessary hydromorphological parameters were predicted for each site based on the fitted hydraulic scaling relationships.

Data analysis

To investigate the underlying processes for gas evasion of both gases, we computed Spearman's correlation between (i) evasion flux and concentration gradient, and (ii) evasion flux and gas specific transfer velocities (using the *rcorr()* function from the R package *Hmisc* version 4.8-0). To compare the importance of the concentration gradient and gas evasion velocity as drivers of evasion flux of the two gases in our dataset, we also computed fractions of explained variance in a multivariate additive model that results from a log-transformation of the diffusive flux equation (4):

$$log\ F_{CH_4} = log\ k_{CH_4} + log\left(C_{CH_4\,w} - C_{CH_4\,EQ}\right) \tag{6}$$

For temporal correlation we examined the data of the three sampling sites used for continuous monitoring. For spatial correlation we considered all measurements taken along the investigated study section at arbitrary times. We further investigated the dynamic range of evasion flux, gas concentration and gas transfer velocity by calculating the coefficient of variance (CV) over space and time.

We did all statistical analyses in R (version 4.1.1) using the *lm()* function for linear regressions and ggplot2 (version 3.3.5) for visualisation. Maps of dissolved gas concentration, gas flux and gas transfer velocity were created using the program QGIS (version 3.28.2).

Results and discussion

Scaling relationships for hydromorphological variables

The investigated river section has no gauging station to monitor discharge or water level. During the field campaign, we observed a stable water level at Ulog and no rainfall. Personal observations of local inhabitants of Ulog confirmed identical conditions during the week prior to our field campaign, which is supported by the nearest meteorological weather station (https://www.wunderground.com/history/daily/ba/sarajevo/LQSA). There is no longer influence of snowmelt at this time of the year (July). We thus assumed constant discharge during our ten-day field campaign at all investigated sites. Discharge ranged from 0.50 m^3 s^{-1} at the most upstream site (above the confluence with Krupac tributary) to 12.27 m^3 s^{-1} close to Glavatićevo (Tab. 1).

We fitted a simple linear model to predict discharge (Q, in $\frac{m^3}{s}$) from the catchment area (A, in km^2) (R^2 = 0.91, with a proportional factor of $10^{-8}\,\frac{m^3}{s\,km^2}$) at any location along the whole investigated river section. Additionally, we used measured hydromorphological variables to fit hydraulic scaling relationships using a linear model with log-transformed variables. We used the root mean square error (RMSE) between model predictions and the measured hydromorphological measurements to compare model parameterisations from our fit and parameters reported in literature (Raymond et al. 2012; Ceola et al. 2014) (Tab. 2). While model parameters reported in Raymond et al. (2012) are derived from a large global dataset and are consequently generalised to predict hydromorphological variables at a larger scale, our parameters, along with parameters from Ceola et al. (2014), were obtained by fitting a single river network. Values for estimated exponents from our study are quite close to values reported from Ceola et al. (2014), who investigated the Ybbs catchment in Austria, which is dominated by calcareous and dolomitic limestone and karstic terrain in the higher mountainous areas. Similarities in our model parameters to parameters from Ceola et al. (2014) can be explained by geological and hydrological similarities of the two catchment areas. Lastly, we used model parameters obtained in this study to compute flow velocity and channel depth along the whole study section.

In an ensemble-modelling approach, we used Q, d and v from our models, in combination with river slope extracted from the DEM, to estimate k_{600} for the whole investigated river section and to identify reaches with high vs. low gas transfer potential (Fig. 3). k_{600} was spatially heterogeneous along the investigated river section, with a high dynamic range (CV of 94 %). This is largely due to variation of slope and results in a few reaches of very high gas transfer velocity (> 100 m d^{-1}), of which two reaches had k_{600} even above 150 m d^{-1}. Compared to these steep reaches, gas transfer in flatter, slower flowing sections was approximately 100 times lower (lowest value of 1.7 m d^{-1}), resulting in a range of k_{600} spanning three orders of magnitude. Mean k_{600} at our sampling sites was 37.6 ± 35.5 m d^{-1}, with a distribution slightly skewed towards higher values (median of 28.8 m d^{-1}) and a maximum value of 164.5 m d^{-1}.

Table 1. Measured hydromorphological variables along the main stem of the Neretva River. Site 1.0 is directly after the confluence with the Krupac tributary and discharge is computed from the mass balance of both tributaries. Depth and flow velocity are reported as mean with standard deviation from a sample size of 15 to 43 measurements.

Tabela 1. Izmerjene hidromorfološke spremenljivke vzdolž glavnega toka reke Neretve. Mesto 1.0 je tik pod sotočjem s pritokom Krupac. Pretok je tu izračunan kot seštevek obeh pritokov. Globina in hitrost toka sta navedeni kot povprečje s standardnim odklonom iz vzorca 15 do 43 meritev.

Tabela 1. Izmjerene hidromorfološke varijable duž glavnog toka rijeke Neretve. Mjesto 1.0 je odmah nakon ušća sa pritokom Krupac i protok je izračunat iz balansa mase obe pritoke. Dubina i brzina toka prikazani su kao prosjek sa standardnom devijacijom iz uzorka veličine od 15 do 43 mjerenja.

Site	Latitude	Longitude	Q ($m^3 s^{-1}$)	Depth (m)	Flow velocity ($m s^{-1}$)
0	43.32240	18.43400	0.50	0.30 ± 0.21	0.30 ± 0.21
1	43.32942	18.42574	0.91	0.27 ± 0.18	0.36 ± 0.18
2	43.36523	18.36999	0.88	0.34 ± 0.36	0.55 ± 0.36
3	43.37887	18.35621	0.81	0.52 ± 0.13	0.22 ± 0.13
4	43.40527	18.32304	1.04	0.54 ± 0.21	0.26 ± 0.21
5	43.42414	18.30837	0.99	0.87 ± 0.32	0.41 ± 0.32
6	43.45800	18.32121	1.04	0.53 ± 0.40	0.40 ± 0.40
7	43.48435	18.27429	5.92	0.59 ± 0.26	0.59 ± 0.26
8	43.48227	18.22665	6.05	0.55 ± 0.22	0.67 ± 0.22
10	43.52945	18.08061	12.27	0.55 ± 0.44	0.59 ± 0.44

Dissolved methane (CH_4) concentrations and fluxes

We identified a single hotspot of high CH_4 concentration in an exceptionally large pool in the section upstream of Ulog (Fig. 4 A). All three measurements taken directly in the pool revealed elevated CH_4 concentrations (0.84, 0.54 and 0.63 μmol L^{-1}) compared to measurements in flowing sections. Notably, methane concentration after the turbulent section immediately following the pool was an order of magnitude lower than in the pool (0.087 μmol L^{-1}). Such spatial clustering of high CH_4 concentrations was previously observed in stream reaches enriched in organic matter and lake transitions, in combination with elevated abundance of methanogens (Crawford et al. 2017). In fact, across various types of streams, highest CH_4 concentrations were reported downstream of eutrophic lakes (Crawford & Stanley 2016). This indicates that a change in flow conditions with a resulting longer residence time and an increased trapping of organic material creates an environment prone to methanogenesis, compared to turbulent and free-flowing river sections.

Mean methane concentration along the entire investigated river section was 0.05 ± 0.15 μmol L^{-1}, with a distribution highly skewed towards lower values (median 0.005 μmol L^{-1}). With the exception of measurements associated with one large natural pool, these concentrations are still mostly above saturation but unexpectedly low for the highly vegetated area that likely generates substantial input of organic carbon (with mean DOC of 0.42 ± 0.08 mg L^{-1} in the study reach; Del Campo et al., this issue). In fact, CH_4 concentrations were within the range reported from low-productivity Alpine headwater streams with poorly developed soils and low DOC (Flury & Ulseth 2019) and other low-order streams (Stanley et al. 2016; Wallin et al. 2018). 12% of our measured values were even undersaturated in terms of CH_4 (given a mean measured atmospheric concentration of 2.07 ± 0.11 ppm), turning the river into a local sink of atmospheric CH_4. The respective locations were evenly spread along the whole study section.

Table 2. Parameters of power law relationships for hydraulic scaling of this study, from Raymond et al. (2012) and from Ceola et al. (2014). The latter fitted w, d and v separately and additionally by constraining the sum of the exponents equal to one (labelled as c). Also reported here are the root mean square error (RMSE) between model prediction (after application of the respective function on our data) and observed data (i.e. the site-mean of respective measurements).

Tabela 2. Parametri razmerij moči za hidravlično skaliranje te študije, vzeti iz Raymond et al. (2012) in Ceola et al. (2014). Slednji so prilagajali w, d in v ločeno in dodatno z omejevanjem vsote eksponentov je enako ena (označeno kot c). V tem primeru je zabeležen tudi koren srednjega kvadrata napake (RMSE) med napovedjo modela (po uporabi ustrezne funkcije na naših podatkih) in opaženimi podatki (tj. povprečjem meritev na posameznem mestu).

Tabela 2. Parametri zakona moći za hidrauličko skaliranje ove studije, iz Raymond et al. (2012) i iz Ceola et al. (2014). Ovi posljednji su prilagodili w, d i v zasebno i dodatno ograničavajući zbir eksponenata da bude jednak jedan (označeno kao c). Također su prikazane greške srednjeg kvadrata (RMSE) između modelne predikcije (nakon primjene odgovarajuće funkcije na naše podatke) i zabilježenih podataka (tj. srednjeg mjesta odgovarajućih mjerenja).

	c_d	e_d	$RMSE_d$	c_v	e_v	$RMSE_v$
This study	-0.804	0.133	0.16	-1.025	0.257	0.09
Raymond et al. (2012)	0.4	0.29	1.43	0.19	0.28	1.11
Ceola et al. (2014)	-1.031	0.285	0.20	-0.935	0.317	0.13
Ceola et al. (2014) (c)	-1.156	0.274	0.21	-1.232	0.288	0.12

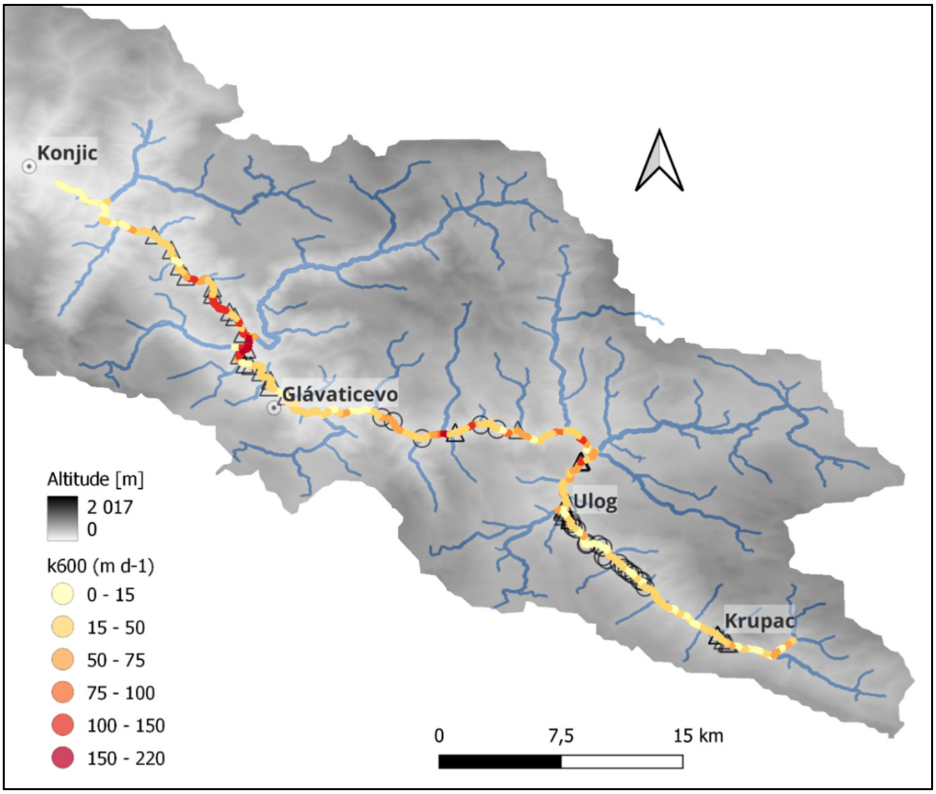

Figure 3. Modelled k_{600} for the whole investigated river section. Sampling sites for discrete gas samples and important locations are shown for orientation.

Slika 3. Modelirani k_{600} za celotni preučevani odsek reke. Za orientacijo so prikazana vzorčišča za posamične vzorce plina in pomembne lokacije.

Slika 3. Modelovani k_{600} za cijeli istraženi dio rijeke. Za orijentaciju su prikazana mjesta uzorkovanja za diskretne uzorke plina i važne lokacije.

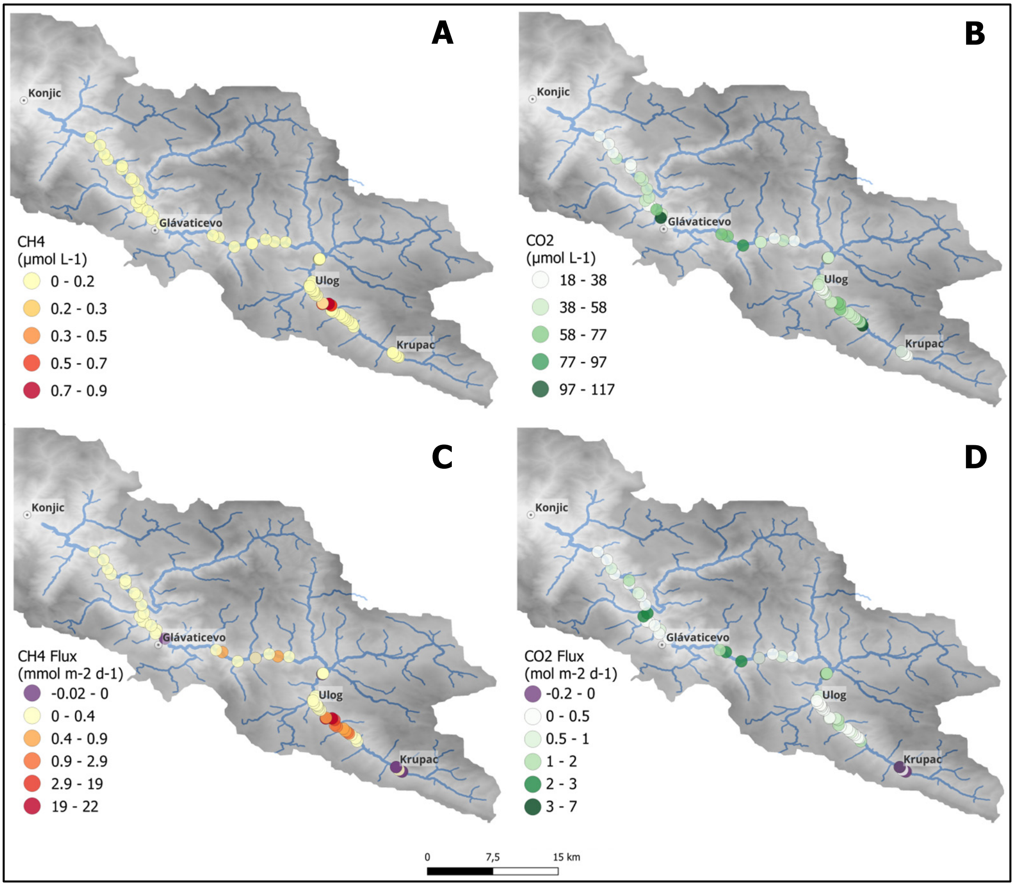

Figure 4. Spatial distribution of CH_4 concentration in µmol L^{-1} (A) and CH_4 Flux (C) as well as CO_2 concentration in µmol L^{-1} (B) and CO_2 Flux (D) along the investigated study section. Locations where the river acted as a sink of atmospheric CH_4 or CO_2 are highlighted as purple dots. Important locations are shown for orientation. Note: CH_4 Flux is given in mmol m^{-2} d^{-1}, while CO_2 Flux in mol m^{-2} d^{-1}.

Slika 4. Prostorska distribucija koncentracije CH4 v µmol L-1 (A) in toka CH_4 (C) ter koncentracije CO_2 v µmol L-1 (B) in toka CO_2 (D) vzdolž preučevanega odseka. Lokacije, kjer je reka delovala kot ponor atmosferskega CH_4 ali CO_2, so označene kot vijolične pike. Za orientacijo so prikazane pomembne lokacije. Opomba: Tok CH_4 je naveden v mmol m^{-2} d^{-1}, medtem ko je tok CO_2 v mol m^{-2} d^{-1}.

Slika 4. Prostorna distribucija koncentracije CH_4 u µmol L-1 (A) i flux CH_4 (C) kao i koncentracija CO_2 u µmol L-1 (B) i flux CO_2 (D) duž istraživanog dijela studije. Mjesta gdje se rijeka ponašala kao ponor atmosferskog CH_4 ili CO_2 označena su ljubičastim tačkama. Za orijentaciju su prikazane važne lokacije. Napomena: CH_4 Flux je dat u mmol m^{-2} d^{-1}., dok je CO_2 Flux u mol m^{-2} d^{-1}.

Our assessment of CH_4 concentration is based on grab samples collected at arbitrary times of the day. This may bias our data given the potential temporal variability and limit comparability across sites. To address this issue, we collected samples over a 24-hour time series at three sites. A clear diurnal cycle was found for CH_4 only at the most downstream of those monitoring sites (Site 10, Fig. 5A), with the highest variation in concentration: temporal coefficients of variation were 35% at Site 10 compared to 26% and 14% at Site 1 and 5, respectively. The highest CH_4 concentration at Site 10 was recorded during morning hours and coincided with lowest temperature and thus highest gas solubility. In fact, the maximum concentration difference at Site 10 was 0.14 µmol L^{-1} (with 0.08 and 0.22 µmol L^{-1} as minimum and maximum values respectively). However, excluding higher concentrations measured at nighttime, when no discrete sampling was done anywhere else, the maximum concentration difference at this site is reduced to 0.04 µmol L^{-1} and the temporal coefficient of variation is reduced from 35% to 16%. For upstream Sites 1 and 5, CH_4 concentration was stable throughout the whole day with mean values of 0.02 ± 0.005 and 0.05 ± 0.007 µmol L^{-1}. Such absence of a strong daily variation in methane concentrations indicates that our grab sample-based measurements are representative even though samples were collected at different daytimes. For further downstream sites, our data suggest caution may be appropriate for estimates of daily mean concentration and evasion fluxes, which may be underestimated given our daytime sampling. However, as all our grab samples were collected during a daytime time window, for which only limited temporal variability could be observed across all sites, we are confident that our data allows unbiased assessment of spatial variation over the whole study section.

Both temporal and spatial variation in CH_4 evasion are strongly correlated to dissolved CH_4 concentration, but not to the gas transfer velocity (Tab. 3). Correlation to concentration becomes even more dominant when data with temporal variation at the three selected monitoring sites are used. Here, minor changes in k_{CH4} result only from changes in water temperature. For spatially variable data, we found ΔC_{CH4} to be the main driver for methane evasion (with R^2 of 0.74 in a simple linear regression), while the river morphology (hence the gas transfer coefficient) had only a minor influence on the amount of gas flux ($R^2 < 0.01$, Fig. 6A). In line with this result, in a multiple linear regression using log-transformed variables, 74% of the variation of CH_4 evasion flux could be attributed to the concentration gradient, but only 16% to the spatially varying gas transfer coefficient. This indicates supply limitation for CH_4 flux in our study system and is further confirmed by CH_4 evasion being at least ten times more variable in space (CV of 353%) than in time (CV of 28, 14 and 33% for Sites 1, 5 and 10 respectively).

The highest evasion flux (22 mmol m^{-2} d^{-1}) was computed at the transition from the large pool with high concentrations to the following turbulent section (Fig. 4C). This is a result of high supply (from CH_4 produced in the pool) and high transfer potential in the downstream flowing section. High CH_4 concentrations are however restricted locally to a couple of hundred meters after their source due to rapid oxidation and/or rapid outgassing. These results are consistent with reported measurements of spatially distinct CH_4 peaks resulting from groundwater input with rapid decline along the consecutive 150 m (Lupon et al. 2019). Additionally, the river can locally act as a sink of atmospheric CH_4 (Fig. 4C).

Mean CH_4 flux to the atmosphere in our study area (1.15 ± 4.06 mmol m^{-2} d^{-1}, computed including sites acting as sinks as well as sources) is within the range reported from mountain headwater streams (Crawford et al. 2015; Stanley et al. 2016; Flury & Ulseth 2019). However, using the mean flux to upscale methane evasion for the whole study area would result in an overestimation of evasion from the system, as high fluxes related to the large pool greatly contribute to a high mean compared to the median CH_4 flux (0.06 mmol m^{-2} d^{-1}).

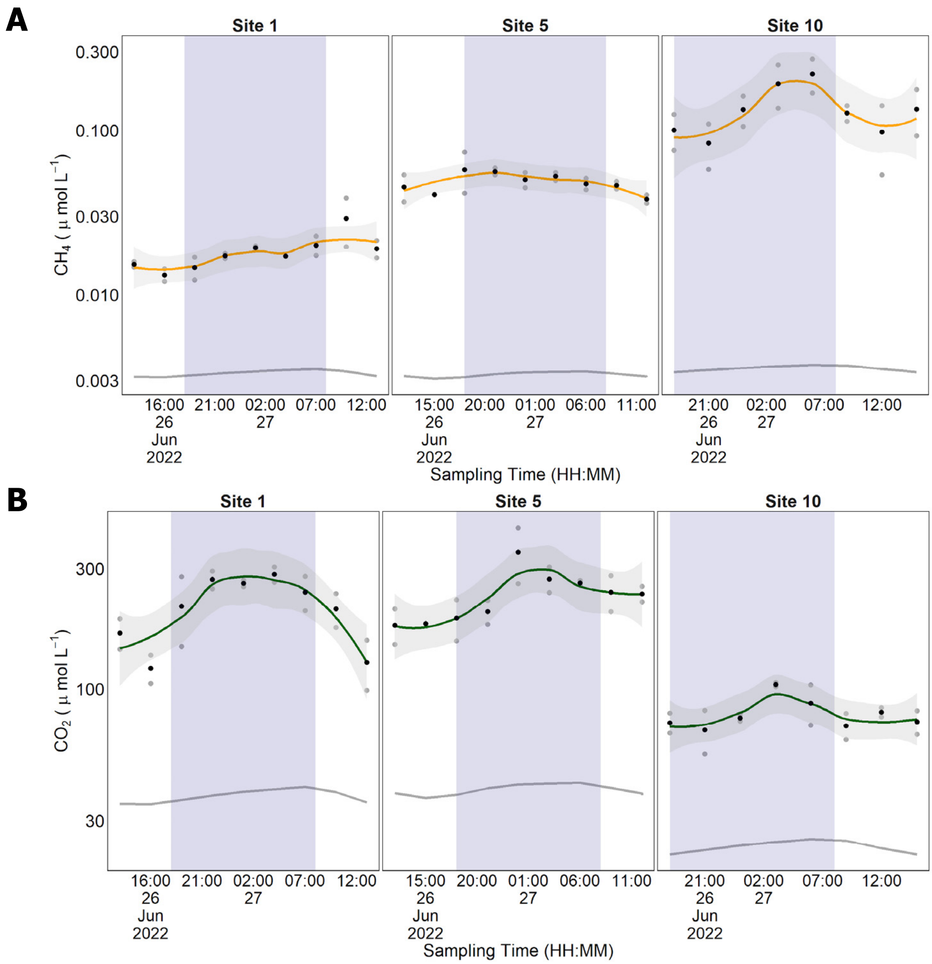

Figure 5. Diurnal concentration trend for CH_4 (A) and CO_2 (B) for Sites 1, 5 and 10. Gray dots represent individual measurements. Black dots represent the average of measurements taken in duplicate. The orange line and green line represent the smoothed trend line using a polynomial regression and the gray area represents the 95% confidence interval of the regression model. The gray line represents the equilibration concentration computed from the atmospheric background and the water temperature. Nighttime, when no samples were taken for discrete gas sample analysis along the continuum, is shaded in blue. Note: The y-axes are in logarithmic scale.

Slika 5. Dnevni trend koncentracije za CH_4 (A) in CO_2 (B) na lokacijah 1, 5 in 10. Sive pike ponazarjajo posamezne meritve, črne pa povprečje podvojenih meritev. Oranžna in zelena črta ponazarjata gladko trendno črto z uporabo polinomske regresije, sivo območje pa 95-odstotni interval zaupanja regresijskega modela. Siva črta predstavlja ravnotežno koncentracijo, izračunano iz atmosferskega ozadja in temperature vode. Nočni čas, ko ni bilo odvzetih vzorcev plina za analizo vzdolž kontinuuma, je modro osenčen. Opomba: osi y so v logaritemski skali.

Slika 5. Dnevni trend koncentracije za CH_4 (A) i CO_2 (B) za mjesta 1, 5 i 10. Sive tačke predstavljaju pojedinačna mjerenja, a crne tačke predstavljaju prosjek mjerenja uzetih u dupliciranim uzorcima. Narandžasta linija i zelena linija predstavljaju izglađenu trend liniju koristeći polinomsku regresiju, a siva oblast predstavlja 95% interval povjerenja regresijskog modela. Siva linija predstavlja koncentraciju ekvilibracije izračunatu iz atmosferske pozadine i temperature vode. Noćno vrijeme, kada se nisu uzimali uzorci za analizu diskretnog plinskog uzorka duž kontinuma, je označeno plavom bojom. Napomena: Y-ose su na logaritamskoj skali.

Dissolved carbon dioxide (CO_2) concentrations and fluxes

Distribution of CO_2 concentration was less skewed towards one side, with mean CO_2 values of 46.4 ± 20.3 and a median of 40.6 µmol L^{-1} (Fig. 4B). Maximum measured CO_2 concentration was 117 µmol L^{-1} and only 7% of measured concentrations were undersaturated compared to the atmosphere (given a mean measured atmospheric concentration of 515 ± 30 ppm). Sites with CO_2-undersaturation were all measured at the upstream end of the study section close to the confluence with the Krupac tributary. Additionally, turbulent sections (with k_{600} ≥ 100 m d^{-1}) generally had lower CO_2 concentrations (maximum of 42 µmol L^{-1}), while less turbulent sections did support a broad range of concentrations (with a variation of 7% with a mean of 40 ± 3 µmol L^{-1} for turbulent and 45% with a mean of 47 ± 21 µmol L^{-1} for less turbulent sections). These findings are supported by aggregated data from a worldwide stream water chemistry data set (Hartmann et al. 2014), where CO_2 concentration was always low at high k_{600} but showed large variations at lower gas transfer velocities.

Table 3. Spearman correlation (and asymptotic p-values) of spatial and temporal variations between evasion flux F_i, stream concentration and gas specific exchange velocities. The i stands for CH_4 for correlation with C_{CH4} and k_{CH4} and for CO_2 for correlation with C_{CO2} and k_{CO2}. For spatial correlation, discrete measurements taken at arbitrary points in time are considered (n=60). For temporal correlation, measurements taken at the three sites of continuous monitoring over 24 hours (each with n=9) are independently analysed and we report mean and standard deviation of correlation coefficients. Changes in k_{CH4} and k_{CO2} on the temporal scale result only from changes in water temperature and were always insignificant.

Tabela 3. Spearmanova korelacija (in asimptotske p-vrednosti) prostorskih in časovnih variacij med tokom emisij Fi, koncentracijo toka in specifičnimi hitrostmi izmenjave plina. i označuje CH4, korelacijo s C_{CH4} in k_{CH4} ter CO_2 za korelacijo s C_{CO2} in k_{CO2}. Pri prostorski korelaciji smo upoštevali posamezne meritve, opravljene ob poljubnem času (n=60). Pri časovni korelaciji smo neodvisno analizirali meritve, opravljene na treh mestih neprekinjenega spremljanja v 24 urah (vsaka z n=9), tu poročamo o povprečju in standardnem odklonu korelacijskih koeficientov. Spremembe v k_{CH4} in k_{CO2} skozi čas so zgolj posledica sprememb v temperaturi vode in so bile vselej neznačilne.

Tabela 3. Spearmanova korelacija (i asimptotske p-vrijednosti) prostornih i vremenskih varijacija između fluxa izbjegavanja Fi, koncentracije toka i specifičnih brzina razmjene gasa. »I« predstavlja CH_4 za korelaciju sa C_{CH4} i k_{CH4} i za CO_2 za korelaciju sa C_{CO2} i k_{CO2}. Za prostornu korelaciju, razmatraju se diskretna mjerenja uzeta u proizvoljnim vremenima (n=60). Za vremensku korelaciju, mjerenja uzeta na 3 mjesta kontinuiranog praćenja tokom 24 sata (svaka sa n=9) se analiziraju nezavisno i prijavljujemo srednju vrijednost i standardnu devijaciju koeficijenata korelacije. Promjene u k_{CH4} i k_{CO2} na vremenskoj skali rezultiraju samo promjenama u temperaturi vode i uvijek su bile nebitne.

		C_{CH4}	k_{CH4}	C_{CO2}	k_{CO2}
Spatial	Corr. Coeff with F_i	0.84	0.08	0.55	0.60
	p	0.00	0.57	0.00	0.42
Temporal	Corr. Coeff with F_i	0.96 ± 0.04	-0.34 ± 0.21	0.96 ± 0.05	-0.57 ± 0.34

At all three sites where gas samples were taken over 24 hours, we found diurnal fluctuations in CO_2 (Fig. 5B), with higher concentrations during nighttime when photosynthesis is absent and respiration prevails. The most downstream site (Site 10) experienced the lowest diurnal fluctuation in CO_2, which might be a result of greater dilution of the benthic primary production signal by the 10-fold higher discharge compared to upstream sites. CO_2 concentration over the investigated time period varied for 29%, 23% and 15% for Sites 1, 5 and 10, respectively, which equals a maximum concentration difference of 164, 170 and 35 µmol L^{-1}. If we consider variation and maximum concentration difference during the restricted sampling window for discrete gas samples (from 08:00 to 18:00) the variation decreases to 26%, 15% and 6% for Sites 1, 5 and 10, respectively and maximum concentration difference is reduced to 86, 63 and 9 µmol L^{-1}. These results indicate that our data supports comparisons of CO_2 concentrations and fluxes across sites of the entire study section, yet daily mean values will suffer from systematic underestimation due to high nighttime CO_2 concentrations.

Evasion of CO_2 was dependent on both ΔC_{CO2} and k_{600}, with R^2 in a simple linear regression of 0.31 and 0.36, respectively (Fig. 6B). In a multiple linear regression using log-transformed variables, 38% of the spatial variation of CO_2 evasion flux could be attributed to the concentration gradient and 62% to the gas transfer coefficient. Compared to spatial variation, temporally variable CO_2 evasion at the three selected sites was strongly correlated to the dissolved concentration rather than to the gas transfer velocity (Tab. 3). This is likely due to high daily variations in the dissolved gas concentration, while on a temporal scale, k_{CO2} changed only due to changes in temperature. Nevertheless, CO_2 evasion was four times more variable in space (CV of 136%) compared to temporal variations at any of the selected three sites (CV of 32, 25 and 18% for Sites 1, 5 and 10 respectively), suggesting external CO_2 point sources and/or locally enhanced mineralization rates as drivers of elevated evasion rates.

Mean computed CO_2 flux among all sampling sites was 0.77 ± 1.04 mol m^{-2} d^{-1} (equal to 9.2 ± 12.5 g_C m^{-2} d^{-1}), with a median of 0.4 and a maximum flux of 6.44 mol m^{-2} d^{-1} (corresponding to 4.8 and 77.3 g_C m^{-2} d^{-1}, respectively). This high flux is a result of the maximum measured CO_2 concentration (117 µmol L^{-1}) spatially co-occurring with an above average k_{600} value (69 m d^{-1}). Although the mean CO_2 evasion is within the range reported from boreal and arctic streams (Lupon et al. 2019; Rocher-Ros et al. 2019), our maximum exceeds the evasion reported from those systems. Uptake of atmospheric carbon, due to undersaturation of the water phase was negligible in our study section.

Conclusion: Hydromorphological implications on GHG concentration and fluxes

Contrary to expected we did not detect any proof for point source input of CH_4 due to groundwater inflow from karstic springs. Influence of point source input on CO_2 concentration cannot be excluded. However, sites with elevated dissolved CO_2 values could not be linked to karstic flow paths. As a result, we found no indication of karstic inputs to dominate GHG concentration and flux patterns in the river continuum in its current pristine form.

We acknowledge that our concentration measurements and computed fluxes represent snapshot estimates taken during hydraulic base flow conditions present during our field campaign in July 2022. A change in flow conditions and extreme hydrological events, can drastically alter the nature and magnitude of GHG emissions from water bodies (Johnson et al. 2007; Dinsmore & Billett 2008). We note that such event-driven pulses cannot be captured with our approach.

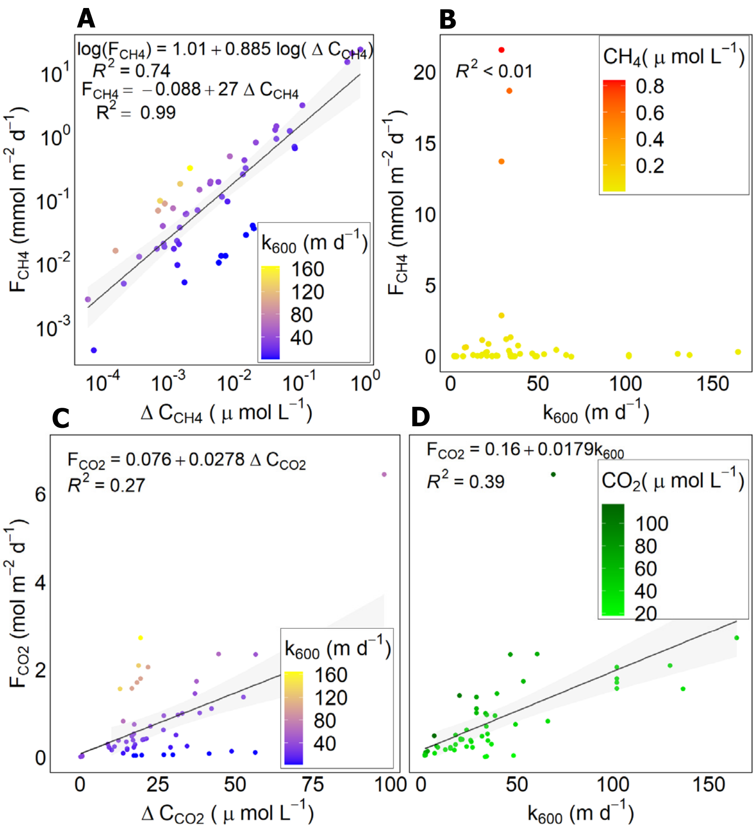

Figure 6. Relationship between CH_4 evasion rate (in mmol m^{-2} d^{-1}) to ΔC_{CH4} (A) and to k_{600} (B) and between CO_2 evasion rate (in mol m^{-2} d^{-1}) to ΔC_{CO2} (C) and to k_{600} (D) in a simple linear regression. ΔC is computed as the difference between dissolved and atmospheric concentration. The black lines represent a linear regression with the gray area showing 95% confidence intervals for the linear model. Fitting parameters are found in the model equation of respective plots. Note: the axes of plot A have a logarithmic scale and model equations for F_{CH4} as function of C_{CH4} are given for log-transformed and non-log transformed values.

Slika 6. Razmerje med stopnjo izparjevanja CH_4 (v mmol m^{-2} d^{-1}) do ΔC_{CH4} (A) in do k_{600} (B) in med stopnjo izparjevanja CO_2 (v mol m^{-2} d^{-1}) do ΔC_{CO2} (C) in do k_{600} (D) v enostavni linearni regresiji. ΔC je izračunan kot razlika med raztopljenimi in atmosferskimi koncentracijami. Črne črte ponazarjajo linearno regresijo, siva območja pa prikazujejo 95-odstotni interval zaupanja za linearni model. Parametre prileganja najdemo v modelni enačbi ustreznih grafikonov. Opomba: osi grafa A so v logaritemski skali, modelne enačbe za F_{CH4} kot funkcijo C_{CH4} pa so podane za logaritemsko transformirane in ne-transformirane vrednosti.

Slika 6. Odnos između stope izbjegavanja CH_4 (u mmol m^{-2} d^{-1}) do ΔC_{CH4} (A) i do k_{600} (B) i između stope izbjegavanja CO_2 (u mol m^{-2} d^{-1}) do ΔC_{CO2} (C) i do k_{600} (D) u jednostavnoj linearnoj regresiji. ΔC je izračunat kao razlika između rastvorene i atmosferske koncentracije. Crne linije predstavljaju linearnu regresiju sa sivom oblasti koja pokazuje 95 % interval povjerenja za linearni model. Parametri prilagođavanja nalaze se u modelnoj jednačini odgovarajućih plotova. Napomena: ose zapleta A su na logaritamskoj skali i modelne jednačine za F_{CH4} kao funkciju C_{CH4} su date za logaritamski transformirane i netransformirane vrijednosti.

Rather than CH_4 originating from groundwater inputs, we found indications that CH_4 is locally produced if conditions allow. Although these two origins are not mutually exclusive, we found a single CH_4 hotspot in an exceptionally large pool upstream of Ulog, where CH_4 concentrations were at least an order of magnitude higher than the measured median for the whole river section. In the pool, standing water and the concomitant increase in residence time in combination with higher sediment and organic matter accumulation likely create a habitat favorable for CH_4 production. As a result of constant CH_4 supply from the pool and high gas transfer velocity due to high water turbulence, evasion of CH_4 was four orders of magnitude higher in the turbulent section immediately following the pool (22 mmol m^{-2} d^{-1} compared to median evasion at network scale of 0.06 mmol m^{-2} d^{-1}). Additionally, CH_4 concentration after this turbulent section was an order of magnitude lower than in the pool, suggesting spatially restricted high outgassing rates, potentially supported by fast CH_4 oxidation. As a result of this single CH_4 hotspot, variation of emissions was an order of magnitude higher in space (353%) than in time (max variation of 33%). On the river network scale, this resulted in the CH_4 concentration to be the critical determinant for spatial variation in CH_4 emissions. The river morphology (hence the gas transfer coefficient) had only little influence on the magnitude of CH_4 flux, indicating a strong supply limitation for CH_4 flux in our study system. In contrast, temporal variation in CO_2 concentration was higher at a diurnal time scale and CO_2 concentration varied widely in space but with less pronounced concentration hot spots. Additionally, sections with high turbulence featured generally lower CO_2 concentrations, while less turbulent sections supported a wider concentration range (with a variation of 7% for turbulent and 45% for less turbulent sections). Spatial variability of CO_2 concentration can originate from external CO_2 and/or heterogeneous sources or accumulation of organic matter, which lead to enhanced mineralisation rates, or from local conditions which favour higher photosynthesis rates. Our results indicate that high CO_2 evasion is due to a combination of both underlying parameters (k_{600} and ΔC_{CO2}) but turbulent reaches can be limited in supply, as the absence of high C_{CO2} in those reaches can be a result of supply rates being lower than evasion rates.

River morphology influences gas transfer potential and although in our study section it had little influence on the magnitude of CH_4 flux, there is no limitation for potential outgassing due to transfer limitation (high dynamic range of k_{600}). However, hydromorphological features play an important role in the creation of environments favoring CH_4 production. Additionally, a change in the flow regime from flowing to standing water also increases possibilities for additional emission pathways (Crawford et al. 2014). Not accounting for these can lead to an underestimation of CH_4 flux of certain features of the river. Converting a free-flowing river reach into a standing water reservoir does not only lead to production and emission of CH_4 instead of CO_2, but also to an activation of additional emission pathways besides diffusion (Maeck et al. 2013; Yang et al. 2014; McGinnis et al. 2016). Specifically, CH_4 ebullition, which can contribute to 80% of emissions in a dammed river (McGinnis et al. 2016) and emissions from periodically inundated riparian vegetation areas must therefore also be considered. These additional emissions are sustained by the trapping of organic material in the reservoir reaches (Maeck et al. 2013). In fact, direct comparison between riverine and reservoir reach revealed the latter to be the major methane source and could directly link these emissions to sediment accumulation even for small dams (Maeck et al. 2013). In alignment with our own findings of high CH_4 fluxes in the turbulent reach immediately downstream of the CH_4-concentration hotspot, reservoirs are known to support high CH_4 fluxes in post-turbine flowing water sections, especially when deeper water bodies are released and brought into contact with the atmosphere (Yang et al. 2014). These mechanisms must be expected to produce higher CH_4 emissions from the Ulog hydropower plant that is currently under construction in the center of our investigated river section.

Povzetek

S kombinacijo meritev vodnega prostora in uporabo sistema za uravnoteženje, ki smo ga izdelali sami, smo lahko določili prostorsko heterogenost koncentracije CH_4 in CO_2 vzdolž 50 km dolgega odseka neokrnjenega rečnega sistema zgornjega toka reke Neretve v Bosni in Hercegovini. Ta odročni del rečnega sistema do sedaj skorajda ni bil izpostavljen človekovim posegom in je, za zdaj, hidromorfološko še vedno nespremenjen v prvotnem naravnem stanju. Za oceno emisij plinov iz lokalnih meritev koncentracije plinov in za oceno dejavnikov zadevnih emisijskih tokov smo uporabili skalirne modele celotnega omrežja za hidromorfološke parametre v kombinaciji z naklonom in povodjem, pridobljenimi iz digitalnega modela višin. Te smo uporabili za izračun hitrosti prenosa plinov. Vzdolž celotnega raziskanega odseka reke smo našli eno žarišče povišane koncentracije CH_4. Visoka koncentracija najverjetneje izvira iz lokalnega nastajanja CH_4, ki je posledica hidromorfoloških razmer, kot je počasi tekoča oziroma stoječa voda, v kateri se kopiči organski material. Tej vroči točki nastajanja CH_4 je sledil turbulenten odsek reke, ki je omogočil visoke tokove izločanja plina. Naši rezultati kažejo, da je izločanje CH_4 v reki Neretvi omejeno z viri. Nasprotno so za izločanje CO_2 odgovorni drugi osnovni mehanistični procesi, ki so bolj spremenljivi v času in prostoru. Na več mestih v preučevanem rečnem odseku se je izločanje CO_2 povečalo, ko sta bila tako k_{600} kot ΔC_{CO2} visoka, kar nakazuje, da ima omejitev prenosa pomembnejšo vlogo poleg oskrbe. Zlasti pri oceni emisij CO_2 dodatno oviro povzroča časovna variabilnost, ki lahko privede do podcenjevanja emisij, če se vzorci jemljejo le podnevi. Naši rezultati tudi poudarjajo pomen diskontinuitete kontrolnih faktorjev za tokove emisij toplogrednih plinov. Hipoteza rečnega kontinuuma, ki ustvarja predvidljiv gradient tokov emisij CO_2 ali CH_4, torej ni podprta v naravni reki, kot je Neretva. Visoki emisijski tokovi katerega koli toplogrednega plina so odvisni od sočasnega pojava fizične priložnosti, ki jo poganja geomorfologija, specifičnih procesov nastajanja toplogrednih plinov ter njihovih virov - habitatov, bogatih z nakopičenim organskim materialom. Kraški izviri bi lahko bili tak vir organskega materiala, ki bi se nadalje presnavljal v reki. Vendar nismo našli znakov, da bi kraški vnosi vplivali na koncentracijo toplogrednih plinov in vzorce pretoka zgornjega toka reke Neretve.

Na splošno lahko rečemo, da emisije toplogrednih plinov preučevanega rečnega odseka trenutno nimajo velikega vpliva na globalno segrevanje. V svojem skoraj naravnem stanju preučevani odsek reke Neretve izpušča večinoma nizke količine CO_2. Edini pomemben vir CH_4 je velik bazen, za katerega je značilna stoječa voda. Projekti hidroelektrarn, načrtovani na tem območju, bi spremenili pogoje pretoka iz tekočih odsekov v velike bazene stoječe vode s podaljšanim časom zadrževanja in kopičenjem organskega materiala. Tudi manjši rezervoarji imajo lahko podobne habitatne pogoje kot opazovana vroča točka CH_4. Posledično pričakujemo višje koncentracije CH_4 in višje emisije CH_4 iz takšnih umetnih, lentičnih okolij kot tudi iz postturbinskih odsekov neposredno nizvodno, kjer se višje hitrosti izmenjave plinov ujemajo z višjimi koncentracijami. Zaradi 28-krat večjega potenciala segrevanja CH_4 v primerjavi s CO_2 bi te spremembe drastično spremenile odtis toplogrednih plinov preučevanega odseka reke Neretve. Spreminjanje hidromorfološkega stanja in toka te naravne reke bo prispevalo h globalnemu segrevanju. Z znanstvenega vidika bi bilo glede na biogeokemične posledice nujno ustaviti razvoj hidroelektrarn na zgornji Neretvi, in namesto tega zaščititi ta rečni odsek kot naravni referenčni sistem, ki nam lahko pomaga izboljšati znanje o vlogi rek v svetovnem ciklu ogljika.

Sažetak

Našom kombinacijom mjerenja vodenog prostora i mjerenja pomoću samostalno izgrađenog ekvilibracijskog sistema, bili smo u mogućnosti otkriti prostornu heterogenost koncentracije CH_4 i CO_2 duž 50 kilometara gornjeg toka rijeke Neretve, izolovanog riječnog sistema koji je do sada bio pod malim uticajem ljudskih aktivnosti. Da bismo procijenili emisije gasa iz lokalnih mjerenja koncentracije gasa i ocijenili pokretače odgovarajućih emisijskih tokova, koristili smo modele mrežnog skaliranja za hidromorfološke parametre u kombinaciji s nagibom i površinom sliva izračunatim iz digitalnog modela elevacije za izračunavanje brzine prenosa gasa. Duž cijelog istraživanog riječnog dijela, pronašli smo jedno žarište povećane koncentracije CH_4. Visoka koncentracija najvjerojatnije potiče iz in situ proizvodnje CH_4, koja je lokalno favorizovana zbog hidromorfoloških uslova, poput sporotekuće do stajaće vode i akumulacije organskog materijala. Ovom žarištu proizvodnje CH_4 slijedilo je turbulentno područje koje omogućava visoke tokove ispuštanja gasova. Naši rezultati stoga sugerišu da je izostajanje CH_4 u rijeci Neretvi snažno ograničeno snabdjevanjem. Suprotno tome, različiti osnovni mehanistički procesi pokreću izostajanje CO_2, koje se pokazalo više varijabilnim u vremenu i prostoru. Izostajanje CO_2 povećalo se kada su na više mjesta u proučavanoj riječnoj dionici bili visoki i k_{600} i ΔC_{CO2}, sugerišući da ograničenje prenosa igra važniju ulogu pored snabdjevanja Pogotovo pri procjeni emisija CO_2, vremenska varijabilnost je dodatna prepreka i može dovesti do potcjenjivanja tokova kada se uzorci uzimaju samo za vrijeme dnevnih sati. Naši rezultati takođe ističu važnost diskontinuiteta kontrolnih faktora za emisije stakleničkih plinova. Ideja o riječnom kontinumu koji stvara predvidljivi gradijent emisija CO_2 ili CH_4 nije podržana u prirodnoj rijeci poput Neretve. Visoki emisijski tokovi bilo kojeg stakleničkog plina zavise o koegzistenciji fizičke prilike pokretane geomorfologijom, podršci procesima proizvodnje i izvora specifičnih za stakleničke plinova koji uključuju staništa bogata akumuliranim organskim materijalom. Kraški izvori mogu dostaviti organski materijal rijeci koji se dalje metabolizira. Međutim, nismo pronašli nikakve indikacije da kraški ulazi utiču na koncentraciju i uzorke tokova stakleničkih plinova gornjeg toka rijeke Neretve. Sveukupno, možemo reći da su emisije stakleničkih plinova proučavanog riječnog dijela trenutno ograničene u smislu njihovog potencijala globalnog zagrijavanja. U svom gotovo prirodnom stanju, proučavani dio rijeke Neretve uglavnom emituje CO_2 pri niskim vrijednostima. Jedini značajan izvor CH_4 je veliki bazen sa stajaćom vodom. Zanimljivo je, hidroenergetski projekti planirani u tom području promijenili bi uslove toka iz tekućih dijelova u velike bazene stajaće vode s povećanim vremenom zadržavanja i akumulacijom organskog materijala. Zapravo, čak bi i manji rezervoari mogli imati slične uslove staništa kao što je promatrano žarište CH_4. Stoga očekujemo veće koncentracije CH_4 i veće tokove snabdjevanja CH_4 iz takvih umjetnih, lentitskih okruženja, kao i iz dijelova neposredno ispod turbine, gdje se veće brzine razmjene gasova podudaraju s većim koncentracijama. Zbog 28 puta većeg potencijala zagrijavanja CH_4 u odnosu na CO_2, ove modifikacije bi drastično promijenile okvir stakleničkih plinova proučavanog dijela rijeke Neretve. Promjena hidromorfološkog stanja i toka ove prirodne rijeke doprinijeće će globalnom zagrijavanju. Sa naučnog stajališta, zaustavljanje izgradnje hidroelektrana na gornjoj Neretvi je čin odgovornosti s obzirom na potencijalne biogeohemijske implikacije. Umjesto toga, bolje bi bilo zaštititi ovaj dio rijeke kao prirodni referentni sistem koji nam može pomoći da poboljšamo naše znanje o ulozi rijeka u globalnom ciklusu ugljenika.

References

Aufdenkampe, AK, Mayorga E, Raymond PA, Melack JM, Doney SC, Alin SR, Aalto RE, Yoo K. 2011. Riverine coupling of biogeochemical cycles between land, oceans, and atmosphere. Frontiers in Ecology and the Environment. 9(1): 53–60. https://doi.org/10.1890/100014

Baker MA, Dahm CN, Valett HM. 1999. Acetate retention and metabolism in the hyporheic zone of a mountain stream. Limnology and Oceanography. 44(6): 1530–1539. https://doi.org/10.4319/lo.1999.44.6.1530

Bastviken D. 2009. Methane. In Encyclopedia of Inland Waters. p. 783–805. Elsevier Inc. https://doi.org/10.1016/B978-012370626-3.00117-4

Butman D, Raymond PA. 2011. Significant efflux of carbon dioxide from streams and rivers in the United States. Nature Geoscience. 4(12): 839–842. https://doi.org/10.1038/ngeo1294

Ceola S, Enrico B, Singer G, Battin TJ, Montanari A, Rinaldo A. 2014. Hydrologic controls on basin-scale distribution of benthic invertebrates. Water Resources Research. 50. https://doi.org/doi:10.1002/2013WR015112

Chamberlain L. 2018. Eco-Masterplan for Balkan Rivers. Drawing a line in the Sand.

Crawford JT, Dornblaser MM, Stanley EH, Clow DW, Striegl RG. 2015. Source limitation of carbon gas emissions in high-elevation mountain streams and lakes. Journal of Geophysical Research: Biogeosciences. 120: 952–964. https://doi.org/10.1002/2014JG002861

Crawford JT, Loken LC, West WE, Crary B, Spawn SA, Gubbins N, Jones SE, Striegl RG, Stanley EH. 2017. Spatial heterogeneity of within-stream methane concentrations. Journal of Geophysical Research: Biogeosciences. 122(5): 1036–1048. https://doi.org/10.1002/2016JG003698

Crawford JT, Stanley EH. 2016. Controls on methane concentrations and fluxes in streams draining human-dominated landscapes. Ecological Applications. 26(5): 1581–1591. https://doi.org/10.1890/15-1330

Crawford JT, Striegl RG, Wickland KP, Dornblaser MM, Stanley EH. 2013. Emissions of carbon dioxide and methane from a headwater stream network of interior Alaska. Journal of Geophysical Research: Biogeosciences. 118(2): 482–494. https://doi.org/10.1002/jgrg.20034

Crawford JT, Stanley EH, Spawn SA, Finlay JC, Loken LC, Striegl RG. 2014. Ebullitive methane emissions from oxygenated wetland streams. Global Change Biology. 20(11): 3408–3422. https://doi.org/10.1111/gcb.12614

Copernicus. 2022. DEM Global and European Digital Elevation Model; [accessed 2022 May 1]. https://doi.org/10.5270/ESA-c5d3d65

Del Campo R, Jechsmayr B, Settles V, Ströder M, Singer G. 2023. Nutrient inputs shape ecosystem functioning gradients along the pristine, upper Neretva River, Bosnia and Herzegovina. Natura Sloveniae. 25(3): 239-263.

DIKTAS B&H. 2012. Protection and Sustainable Use of the Dinaric Karst Transboundary Aquifer System. https://docslib.org/doc/9481960/protection-and-sustainable-use-of-the-dinaric-karst-transboundary-aquifer-system

Dinsmore KJ, Billett MF. 2008. Continuous measurement and modeling of CO2 losses from a peatland stream during stormflow events. Water Resources Research. 44(12). https://doi.org/10.1029/2008WR007284

Djedjibegovic, J, Marjanovi A, Sober M, Skrbo A, Sinanovic K, Larssen T et al. 2010. Levels of persistent organic pollutants in the Neretva River (Bosnia and Herzegovina) determined by deployment of semipermeable membrane devices (SPMD). Journal of environmental science and health, Part B. 45: 128–136.

Drake TW, Raymond PA, Spencer RGM. 2018. Terrestrial carbon inputs to inland waters: A current synthesis of estimates and uncertainty. Limnology and Oceanography Letters. 3(3): 132–142. https://doi.org/10.1002/lol2.10055

Duvert C, Butman DE, Marx A, Ribolzi O, Hutley LB. 2018. CO2 evasion along streams driven by groundwater inputs and geomorphic controls. Nature Geoscience. 11(11): 813–818. https://doi.org/10.1038/s41561-018-0245-y

Flury S, Ulseth AJ. 2019. Exploring the Sources of Unexpected High Methane Concentrations and Fluxes From Alpine Headwater Streams. Geophysical Research Letters. 46(12): 6614–6625. https://doi.org/10.1029/2019GL082428

Gómez-Gener L, Rocher-ros G, Battin T, Cohen MJ, Dalmagro HJ, Dinsmore KJ, Drake TW, Duvert C, Enrich-prast A, Horgby Å, Johnson MS, Kirk L, Machado-silva F, Marzolf NS, Mcdowell MJ, Mcdowell WH, Miettinen H, Ojala AK, Peter H, … Six, J. 2021. Global carbon dioxide efflux from rivers enhanced by high nocturnal emissions. Nature Geoscience. 14(5). https://doi.org/10.1038/s41561-021-00722-3

Grego J. 2020. Revision of the stygobiont gastropod genera *Plagigeyeria* (Tomlin, 1930) and *Travunijana* (Grego an Glöer, 2019) (Mollusca; Gastropoda; Moitessieriidae and Hydrobiidae) in Hercegovina and adjacent regions. European Journal of Taxonomy. 2020(691): 1–56. https://doi.org/10.5852/EJT.2020.691

Hartmann J, Lauerwald R, Moosdorf N. 2014. A brief overview of the GLObal RIver Chemistry Database. GLORICH. Procedia Earth and Planetary Science. 10: 23–27. https://doi.org/10.1016/j.proeps.2014.08.005

Horgby Å, Boix Canadell M, Ulseth AJ, Vennemann TW, Battin TJ. 2019. High-resolution spatial sampling identifies groundwater as driver of CO_2 dynamics in an alpine stream network. Journal of Geophysical Research: Biogeosciences. 124(7): 1961–1976. https://doi.org/10.1029/2019JG005047

Hotchkiss ER, Hall RO, Sponseller RA, Butman D, Klaminder J, Laudon H, Rosvall M, Karlsson J. 2015. Sources of and processes controlling CO_2 emissions change with the size of streams and rivers. Nature Geoscience. 8(9): 696–699. https://doi.org/10.1038/ngeo2507

[IHA] International Hydropower Association. 2010. GHG measurement guidelines for freshwater reservoirs. Editor Joel A. Goldenfum. International Hydropower Association, London, UK.

Jähne B, Heinz G, Dietrich W. 1987. Measurement of the diffusion coefficients of sparingly soluble gases in water. Journal of Geophysical Research. 92(C10): 10767. https://doi.org/10.1029/JC092iC10p10767

Johnson MS, Weiler M, Couto EG, Riha SJ, Lehmann J. 2007. Storm pulses of dissolved CO_2 in a forested headwater Amazonian stream explored using hydrograph separation. Water Resources Research. 43(11). https://doi.org/10.1029/2007WR00635

Leach JA, Lidberg W, Kuglerová L, Peralta-Tapia A, Ågren A, Laudon H. 2017. Evaluating topography-based predictions of shallow lateral groundwater discharge zones for a boreal lake-stream system. Water Resources Research. 53(7): 5420–5437. https://doi.org/10.1002/2016WR019804

Ledesma JLJ, Futter MN, Blackburn M, Lidman F, Grabs T, Sponseller RA, Laudon H, Bishop KH, Köhler SJ. 2018. Towards an improved conceptualization of riparian zones in boreal forest headwaters. Ecosystems. 21(2): 297–315. https://doi.org/10.1007/s10021-017-0149-5

Leopold L, Wolman M, J M. 1964. Fluvial processes in geomorphology.

Lupon A, Denfeld BA, Laudon H, Leach J, Karlsson J, Sponseller RA. 2019. Groundwater inflows control patterns and sources of greenhouse gas emissions from streams. Limnology and Oceanography. 64(4): 1545–1557. https://doi.org/10.1002/lno.11134

Maeck A, Delsontro T, McGinnis DF, Fischer H, Flury S, Schmidt M, Fietzek P, Lorke A. 2013. Sediment trapping by dams creates methane emission hot spots. Environmental Science and Technology. 47(15): 8130–8137. https://doi.org/10.1021/es4003907

McGinnis DF, Bilsley N, Schmidt M, Fietzek P, Bodmer P, Premke K, Lorke A, Flury S. 2016. Deconstructing methane emissions from a small Northern European river: hydrodynamics and temperature as key drivers. Environmental Science and Technology. 50(21): 11680–11687. https://doi.org/10.1021/acs.est.6b03268

Operta M, Pamuk S. 2015. Geological characteristics and tectonic structure of the upper Neretva basin. Acta geographica Bosniae et Herzegovinae. p. 63–74.

Peter H, Singer GA, Preiler C, Chifflard P, Steniczka G, Battin TJ. 2014. Scales and drivers of temporal pCO_2 dynamics in an Alpine stream. Journal of Geophysical Research: Biogeosciences. 119(6): 1078–1091. https://doi.org/10.1002/2013JG002552

Rasilo T, Hutchins RHS, Ruiz-González C, del Giorgio PA. 2017. Transport and transformation of soil-derived CO_2, CH_4 and DOC sustain CO_2 supersaturation in small boreal streams. Science of the Total Environment. 579: 902–912. https://doi.org/10.1016/j.scitotenv.2016.10.187

Raymond PA, Hartmann J, Lauerwald R, Sobek S, McDonald C, Hoover M, Butman D, Striegl R, Mayorga E, Humborg C, Kortelainen P, Dürr H, Meybeck M, Ciais P, Guth P. 2013. Global carbon dioxide emissions from inland waters. Nature. 503(7476): 355–359. https://doi.org/10.1038/nature12760

Raymond PA, Zappa CJ, Butman D, Bott TL, Potter J, Mulholland P, Laursen AE, McDowell WH, Newbold D. 2012. Scaling the gas transfer velocity and hydraulic geometry in streams and small rivers. Limnology and Oceanography: Fluids and Environments. 2(1): 41–53. https://doi.org/10.1215/21573689-1597669

Rocher-Ros G, Sponseller RA, Lidberg W, Mört, C, Giesler R. 2019. Landscape process domains drive patterns of CO 2 evasion from river networks. Limnology and Oceanography Letters. 4(4): 87–95. https://doi.org/10.1002/lol2.10108

Stanley EH, Casson NJ, Christel ST, Crawford JT, Loken LC, Oliver SK. 2016. The ecology of methane in streams and rivers: patterns, controls, and global significance. Ecological Monographs. 86(2): 146–171. https://doi.org/10.1890/15-1027

Talluto MV. 2020. WatershedTools: An R package for the spatial analysis of watersheds. version 0.4.9, https://github.com/flee-group/watershed

Valdes D, Dupont JP, Laignel B, Ogier S, Leboulanger T, Mahler BJ. 2007. A spatial analysis of structural controls on Karst groundwater geochemistry at a regional scale. Journal of Hydrology. 340(3–4): 244–255. https://doi.org/10.1016/j.jhydrol.2007.04.014

Wallin MB, Campeau A, Audet J, Bastviken D, Bishop K, Kokic J, Laudon H, Lundin E, Löfgren S, Natchimuthu S, Sobek S, Teutschbein C, Weyhenmeyer GA, Grabs T. 2018. Carbon dioxide and methane emissions of Swedish low-order streams—a national estimate and lessons learnt from more than a decade of observations. Limnology and Oceanography Letters. 3(3): 156–167. https://doi.org/10.1002/lol2.10061

Wilkinson J, Bors C, Burgis F, Lorke A, Bodmer P. 2018. Measuring CO 2 and CH 4 with a portable gas analyzer: Closed-loop operation, optimization and assessment. PLoS ONE. 13(4): 1–16. https://doi.org/10.1371/journal.pone.0193973

Xiao S, Liu L, Wang W, Lorke A, Woodhouse J. 2020. A Fast-Response Automated Gas Equilibrator (FaRAGE) for continuous in situ measurement of CH_4 and CO_2 dissolved in water. Hydrology and Earth System Sciences. 24(7): 3871–3880. https://doi.org/10.5194/hess-24-3871-2020

Yang L, Lu F, Zhou X, Wang X, Duan X, Sun B. 2014. Progress in the studies on the greenhouse gas emissions from reservoirs. Acta Ecologica Sinica. 34(4): 204–212. https://doi.org/10.1016/j.chnaes.2013.05.01